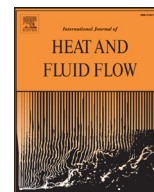




Contents lists available at ScienceDirect

International Journal of Heat and Fluid Flow

journal homepage: www.elsevier.com/locate/ijheatfluidflow

Transition control in a three-dimensional boundary layer by direct attenuation of nonlinear crossflow vortices using plasma actuators

P.C. Dörr, M.J. Kloker*

Institut für Aerodynamik und Gasdynamik, Universität Stuttgart, Pfaffenwaldring 21, D-70550 Stuttgart, Germany

ARTICLE INFO

Article history:

Received 12 November 2015

Revised 24 March 2016

Accepted 7 June 2016

Available online xxx

Keywords:

Transition to turbulence

Instability control

Crossflow vortices

Plasma actuators

Direct numerical simulations

ABSTRACT

Direct numerical simulations are used to probe the potential of plasma actuators to attenuate nonlinear steady crossflow vortices (CFVs). The investigated base flow mimics the three-dimensional boundary-layer flow of a swept wing. The plasma actuators are positioned at selected spanwise positions to weaken oncoming CFVs and thus the associated (secondary) instability. It is shown that both volume forcing against or in the direction of the crossflow (CF) can be effective, and a significant transition delay can be achieved. The spanwise position of the actuators should be such that the actuation-induced downdraft inhibits the CFV. The forcing in the direction of the CF does not reduce the mean CF, and an unfavourable spanwise position of the actuator may directly increase the strength of the CFV and eventually promote turbulence onset. The forcing against the CF never turned out to promote turbulence onset for all investigated positions, because of the favourable reduction of the mean CF. Adding then a second or third actuator downstream at appropriate spanwise positions can yield enhanced transition delay.

© 2016 Elsevier Inc. All rights reserved.

1. Introduction

Increasing the efficiency of future aircraft and aerodynamic devices is a vital task for both environmental and economic reasons. Due to limited potential in further improvement of shaping, surface quality and engines, a promising approach is to extend the regions of laminar flow on aerodynamic surfaces by hybrid laminar flow control (HLFC). Caused by the leading-edge sweep of aircraft wings and stabilisers, distinctly three-dimensional boundary layers develop and their transition from laminar to turbulent flow is typically dominated by crossflow (CF) instability. Primary CF instability leads to growth of steady and travelling crossflow vortex (CFV) modes. At cruise conditions, steady CFV modes excited by surface roughness typically prevail and streamwise orientated, co-rotating CFVs are formed. They generate localised high-shear layers, triggering a strong secondary instability rapidly invoking turbulence. Detailed studies were performed in the last decades to understand the transition process including the secondary instability, see, e.g., Bippes (1999), Koch et al. (2000), Malik et al. (1999), Saric et al. (2003), Wassermann and Kloker (2002, 2003).

Since the 1950s, slot- or hole-panel suction systems have successfully been used in prototype studies to delay transition, based on a reduction of the CF velocity and consequently primary CF

instability. Detailed overview articles on experiments and flight campaigns are given by Joslin (1998a, 1998b). The most important results have been summarised by Messing and Kloker (2010). More recently other methods to control the CF dominated transition process have been developed. Saric et al. (1998) and Saric and Reed (2002) used a spanwise row of roughness elements (distributed-roughness-elements, DRE). These elements excite steady 'subcritical' CFV modes that are spaced narrower than the most amplified mode and induce a useful mean-flow distortion. As a consequence, the naturally growing most amplified mode is hindered in growth. The control mode eventually decays or causes no secondary instability, and transition to turbulence is delayed; see also Hosseini et al. (2013). The same concept, however named upstream-flow-deformation (UFD) and not necessarily based on roughness elements, was suggested by Wassermann and Kloker (2002) using direct numerical simulations (DNS). An approach combining classical suction with the UFD concept was proposed by Kloker (2008) and Messing and Kloker (2010), named distributed flow deformation (DFD) or formative suction. They designed suction orifice panels that continuously generate and maintain locally optimal narrow-spaced CFVs. These CFVs do not cause secondary instability and suppress the most unstable steady modes. Bonfigli and Kloker (2007) detected a strong sensitivity of the amplification of secondary instability modes with respect to the definition of the wall-normal velocity component of the underlying base flow, and consequently Friederich and Kloker (2008, 2012) developed the 'pinpoint-suction' concept. It is applied to directly target the

* Corresponding author. Tel.: +4971168563427.

E-mail addresses: doerr@iag.uni-stuttgart.de (P.C. Dörr), kloker@iag.uni-stuttgart.de (M.J. Kloker).<http://dx.doi.org/10.1016/j.ijheatfluidflow.2016.06.005>

0142-727X/© 2016 Elsevier Inc. All rights reserved.

three-dimensional nonlinear disturbance state with steady CFVs. By using localised strong suction through holes at the updraft side of the CFVs, the vortical motion is hindered and consequently the secondary instability is weakened or suppressed.

Plasma actuators are an alternative to roughness elements or blowing/suction systems with the benefit of being fully electronic and without moving parts. They are easily flush-mountable and generate a body force that locally accelerates the surrounding fluid. The detailed review articles by Moreau (2007), Corke et al. (2010) and Benard and Moreau (2014) summarise the actuators' working principle and ongoing research. So far, application of plasma actuators for (H)LCF mainly concentrated on two-dimensional, spanwise symmetric boundary-layer flows. Successful transition delay was achieved in experiments, flight tests and numerical simulations. Different control methods were applied, such as (i) the stabilisation of the longitudinal velocity profile, see e.g., Duchmann et al. (2014), Grundmann and Tropea (2007), Riherd and Roy (2013), Séraudie et al. (2011), Vieira (2013), (ii) the active cancellation of T-S waves, see e.g., Grundmann and Tropea (2008), Kotsonis et al. (2013), Kurz et al. (2014), Vieira (2013), (iii) the damping of boundary-layer streaks, see Hanson et al. (2014, 2010), Riherd and Roy (2014), or (iv) the spanwise modulation of the flow field, see Barckmann et al. (2015). The formation of streamwise vortices/streaks in a two-dimensional boundary-layer flow by plasma vortex generators has been investigated in detail by Jukes and Choi (2013). Recently, Dörr and Kloker (2015b) numerically demonstrated the applicability of plasma actuators to stabilise a three-dimensional boundary-layer flow by base-flow manipulation. Similar to the application of suction, the actuators are used to weaken the primary CF instability, mainly due to a reduction of the basic CF. Schuele et al. (2013) experimentally studied the excitability of stationary CFV modes by 'active roughness' produced by an azimuthal array of micrometre-sized plasma actuators. They investigated a three-dimensional Mach 3.5 boundary layer of a sharp-tipped right-circular cone at 4.2° angle of attack. Stationary subcritical CFV modes were successfully excited, hindering the growth of the naturally most amplified mode by the DRE/UFD principle.

The current work investigates the potential of dielectric barrier discharge (DBD) plasma actuators to attenuate nonlinear steady CFVs. The plasma actuators are positioned at selected spanwise positions relative to the oncoming CFVs to weaken them and thus the associated (secondary) instability. The effect of the plasma actuators is modelled by a localised body force using an empirical model with velocity-information-based force-term estimation, see Kriegseis et al. (2013), Maden et al. (2013).

The paper is structured as follows: The numerical method is described in Section 2 and the base flow and its stability characteristics are covered in Section 3. In Section 4 control results are shown using one actuator per fundamental spanwise wavelength. Various actuator configurations with forcing either against or in the direction of the CF are studied in detail in Section 4.1. Further investigations on forcing against the CF, varying the electrode length, the body-force amplitude and the number of actuators positioned along the CFV, are presented in Section 4.2. In Section 5 the results for a set-up using two actuators per fundamental spanwise wavelength with forcing against the CF are shown.

2. Numerical method

2.1. Basic set-up

The DNS are performed with the in-house code NS3D. The code is proven for the investigation of the CFV-induced laminar breakdown, see Dörr and Kloker (2015b), Friederich and Kloker (2012), Kurz and Kloker (2014). It solves the three-dimensional, unsteady, compressible Navier–Stokes equations together with the

continuity and energy equation in conservative formulation. $Q = [\rho, \rho u, \rho v, \rho w, \rho e]^T$ represents the non-dimensional solution vector, where ρ and e are the density and the total energy, respectively. The velocity vector $u = [u, v, w]^T$ denotes the velocities in the chordwise, wall-normal and spanwise directions x , y and z , respectively. Velocities and length scales are normalised by the chordwise reference velocity \bar{U}_∞ and the reference length \bar{L} , respectively. The overbar denotes dimensional values. Additionally, the reference temperature \bar{T}_∞ and the reference density $\bar{\rho}_\infty$ are used for normalisation. The specific heats c_p and c_v as well as the Prandtl number are assumed to be constant. The temperature dependence of the viscosity μ is modelled by Sutherland's law. A rectangular integration domain on a flat plate is considered for the simulations, see Fig. 1. The domain consists of block-structured Cartesian grids. The chordwise and wall-normal directions are discretised using mainly 8th-order explicit or 6th-order compact finite differences. For the spanwise direction a Fourier-spectral ansatz is implemented to compute the z -derivatives. The classical fourth-order Runge–Kutta scheme is used for time integration. For more details see also Babucke et al. (2006).

The considered base flow mimics the set-up of the DLR-Prinzipexperiment Göttingen, see e.g. Bippes (1999), Bonfigli and Kloker (2007). It consists of a flat plate with an effective sweep angle Φ_∞ of 42.5° and a displacement body above the plate to obtain a nearly constant favourable chordwise pressure-gradient with Hartree parameter $\beta_H = 2/3$. The chordwise free-stream velocity $\bar{U}_{\infty, \text{exp}}$ was 14 m s⁻¹ in the experiments, yielding a chordwise Mach number $Ma_{\infty, \text{exp}} = 0.04$. The viscous part of the numerical time-step limit typically dominates for such small Mach numbers, and a time step proportional to Ma_∞^2 is then enforced. To allow calculations at a non-prohibitive time step, $Ma_\infty = 0.21$ is chosen for the present simulations. For this Mach number both the temperature T_B and the density ρ_B of the base flow vary by less than 2.1% within the integration domain, indicating quasi-incompressible flow behaviour. By matching the Reynolds-numbers based on the displacement thickness δ_1 flow similarity is ensured. The reference values are $\bar{T}_\infty = 303.4\text{ K}$ and $\bar{\rho}_\infty = 1.225\text{ kg m}^{-3}$. Like for the experiments, the reference velocity \bar{U}_∞ is chosen at a flow angle of $\Phi_\infty = 42.5^\circ$, yielding $\bar{U}_\infty = \bar{w}_e / \tan \Phi_\infty = 72.72\text{ m s}^{-1}$, where \bar{w}_e is the spanwise velocity at the upper boundary of the integration domain. At kept global Reynolds number $Re = 92000$ based on \bar{U}_∞ and \bar{L} , the reference length is $\bar{L} = 0.01923\text{ m}$ ($\bar{L}_{\text{exp}} = 0.1\text{ m}$). An extensive description of the base-flow computation and a comparison to the incompressible base flow is provided by Friederich and Kloker (2012).

An equally spaced grid with 2560 points is used to discretise the chordwise direction, with $1.900 \leq x \leq 5.249$ and $\Delta x = 1.309 \cdot 10^{-3}$. In the wall-normal direction a stretched grid with 105 points is used, $\Delta y_{\text{wall}} = 2.300 \cdot 10^{-4}$, and $0.000 \leq y \leq 0.099$ with $\delta_1(x_0) = 0.0054$. To save computational costs, a smaller domain is cut out of the original domain for the baseline cases shown in Section 4.1. This domain covers $1.900 \leq x \leq 4.386$ (1900 points), and $0.000 \leq y \leq 0.073$ (93 points). In the spanwise direction the fundamental wavelength is $\lambda_{z,0} = 0.126$, corresponding to the fundamental spanwise wavenumber $\gamma_0 = 2\pi/\lambda_{z,0} = 50.0$. It is discretised with 64 points ($K = 21$ de-aliased Fourier modes), yielding $\Delta z = 1.964 \cdot 10^{-3}$. The time step Δt is set to $1.575 \cdot 10^{-5}$, and the reference angular frequency is $\omega_0 = 6.0$. The following boundary conditions are used: At the inflow, all base-flow variables are prescribed and upstream-travelling acoustic waves are allowed to leave the integration domain using characteristic conditions for the disturbances. At the isothermal wall, the no-slip boundary condition using $dp/dy|_{\text{wall}} = 0$ for the wall pressure is employed. The density is calculated from the equation of state, and the temperature is $\bar{T}_{\text{wall}} = \bar{T}_\infty = 303.4\text{ K}$. In the outflow region a buffer domain is used where all conservative variables are damped back to the

Download English Version:

<https://daneshyari.com/en/article/4993349>

Download Persian Version:

<https://daneshyari.com/article/4993349>

[Daneshyari.com](https://daneshyari.com)